Comparative Study on Inorganic Composition and Crystallographic Properties of Cortical and Cancellous Bone[1]

XIAO-YAN WANG, YI ZUO, DI HUANG, XIAN-DENG HOU, AND YU-BAO LI[2]

Research Center for Nano-Biomaterials Analysis and Testing, Sichuan University, Chengdu 610064, Sichuan, China

Objective To comparatively investigate the inorganic composition and crystallographic properties of cortical and cancellous bone via thermal treatment under 700 ℃. **Methods** Thermogravimetric measurement, infrared spectrometer, X-ray diffraction, chemical analysis and X-ray photo-electron spectrometer were used to test the physical and chemical properties of cortical and cancellous bone at room temperature 250 ℃, 450 ℃, and 650 ℃, respectively. **Results** The process of heat treatment induced an extension in the *a*-lattice parameter and changes of the *c*-lattice parameter, and an increase in the crystallinity reflecting lattice rearrangement after release of lattice carbonate and possible lattice water. The mineral content in cortical and cancellous bone was 73.2wt% and 71.5wt%, respectively. For cortical bone, the weight loss was 6.7% at the temperature from 60 ℃ to 250 ℃, 17.4% from 250 ℃ to 450 ℃, and 2.7% from 450 ℃ to 700 ℃. While the weight loss for the cancellous bone was 5.8%, 19.9%, and 2.8 % at each temperature range, the Ca/P ratio of cortical bone was 1.69 which is higher than the 1.67 of stoichiometric HA due to the B-type CO_3^{2-} substitution in apatite lattice. The Ca/P ratio of cancellous bone was lower than 1.67, suggesting the presence of more calcium deficient apatite. **Conclusion** The collagen fibers of cortical bone were arrayed more orderly than those of cancellous bone, while their mineralized fibers ollkded similar. The minerals in both cortical and cancellous bone are composed of poorly crystallized nano-size apatite crystals with lattice carbonate and possible lattice water. The process of heat treatment induces a change of the lattice parameter, resulting in lattice rearrangement after the release of lattice carbonate and lattice water and causing an increase in crystal size and crystallinity. This finding is helpful for future biomaterial design, preparation and application.

Key words: Cortical bone; Cancellous bone; Bone mineral; Composition; Crystallographic property

INTRODUCTION

Mineral, collagen, and water are the major components of natural fresh bone, in which the total organic matrix, water and carbonate account for about 25 wt%, 9.7 wt%, and 5.8 wt%, respectively. The mineral as the main part of natural bone is composed of nano apatite crystals (-25nm in length), which is about 60 wt% in fresh bone and 70 wt% in dry bone. Compared with sintered HA ceramic, the crystallinity of bone apatite is only 33%-37%[1]. The carbonate ion is known as a substitute both for OH (Type A substitution) and phosphate groups (Type B substitution) in the apatite crystal structure[2].

Water in bone exists in cells, fluid, collagen, and bone mineral-apatite crystals. The interaction of water with mineral and collagen is critical to the mechanical behavior of fresh bone[3]. There are many types of water which are present in bone[4-7], such as free water, the structural water forming hydrogen bonds within the triple helix of collagen molecules and crystal water bonding to apatite surface or in the crystal lattice, etc. Evidence for an architecture and distribution of water in bone by nuclear magnetic resonance (NMR) has recently been published[8-11]. The release of water from hard tissues is a continuous and gradual process involving the breakage of hydrogen bonds formed by loosely and strongly bound water and water diffusion out of the biological system[12]. The energy to remove water is in the following order: free water <water loosely bound to surface of collagen <water trapped inside collagen molecules <water bound to surface of mineral apatite <water imbedded in the lattice of apatite <structural water in collagen[13]. According to the results of previous researches, the free water and loosely bound water can be released easily

[1]This work is supported by China 973 Fund (No.2007CB936102) and the National Natural Science Foundation of China (No. 50972096).

[2]Correspongdence should be addressed to Yu-Bao LI. Tel: 86-28-85412847. Fax: 86-28-85417273. E-mail: nic7504@scu.edu.cn

Biographical note of the first author: Xiao-Yan WANG, female, born in 1980, research assistant, Ph D candidate in Sichuan University, majoring in Biomedical Engineering.

0895-3988/2010
CN 11-2816/Q

and water bound to surface of crystals is lost at a temperature below 200 ℃[14].

Because of the poor crystallinity of bone apatite, determination of its characteristics deduced from diffractomeric techniques is complicated. Most researches on the X-ray diffraction of heat treated or burned bone are focused on the variation of composition and crystallinity at high temperature (700-1 300 ℃)[15-18]. In the high temperature range, water, carbonate and collagen have been fully removed. These investigations are based on the fact that the heated bones cause a sharpening of diffraction patterns, contributing to the increased crystallite size and rearrangement of bone apatite. However, little attention has been paid to comparative study on inorganic composition and crystallographic properties of cortical and cancellous bone under 700 ℃. It is natural to expect that systematic and detailed structural studies of the bone mineral will lead to a better understanding of its effect on the physical and biological properties of natural bone. Furthermore, it can provide useful data for the design and development of biomaterials dedicated to the repair and replacement of bone and to the induction of bone formation.

In this paper, porcine cortical bone and cancellous bone were processed as specimens and treated at 250 ℃, 450 ℃, and 650 ℃, respectively. Different analytical methods were used to investigate the microstructure, weight change accompanying the release of water of different types and lattice carbonate with increasing temperature, phase composition and crystallinity, apatite crystal size and lattice parameters, as well as the element binding energy. The investigation will be helpful for future biomaterial design, preparation and application.

MATERIALS AND METHODS

Sample Preparation

As the porcine bone is much similar to human bone, the femurs of mature healthy pigs were chosen to prepare the specimens. Before section, the periosteum and endosteum were removed to obtain the bone fragments including cortical and cancellous bone. The diaphysis fragments were sectioned in 1 mm slice, washed with acetone for 3 times and deionized water for 3 times, and boiled in $CHCl_3/CH_3OH$ (3/1, v/v) solution for 24 h to remove lipid. The degreased samples were washed with deionized water and heated at 90 ℃ for 24 h, then cooled to room temperature. Powder samples were also prepared by grinding in an agate mortar and sieved *via* 220-mesh.

The cortical and cancellous parts of the bone section were separated as a pair of specimen, and these samples were sintered in a muffle furnace at temperatures of 250 ℃, 450 ℃, and 650 ℃, respectively by a heating rate of 0.05 ℃/s and kept at the target temperature for 4h. After heat treatment, the samples were cooled down to the room temperature in a desiccator. The samples of cortical bone (CO) and cancellous bone (CA) dehydrated at 250 ℃, 450 ℃, 650 ℃ were abbreviated for CO250, CO450, CO650, and CA250, CA450, and CA650, respectively.

SEM Observation

The surface morphologies of the cortical and cancellous bone slices were observed by scanning electron microscopy (SEM, HITACHI S3 400, Japan) at 20 kV after surface gold sputtering. The bone sections were fixed with 1% volume fraction of glutaraldehyde, subjected to graded alcohol dehydration, rinsed with isoamyl acetate and dried at critical point.

TG Analysis

Thermogravimetric (TG) measurements were performed with a Netzsch TG 209 F1 instrument (Netzsch, Germany) in nitrogen atmosphere. TG curves were taken in the range of 40 ℃ to 700 ℃ at a heating rate of 10 ℃/min.

XRD Analysis

The powders of cortical and cancellous bone were tested by an X-ray diffractometer (XRD, X'Per Pro MPD, Philips, The Netherlands) with Cu Kα radiation (λ=0.154 nm). Each sample was scanned at 2θ from 10 ° to 60 ° with a scanning rate of 3 °·min^{-1}. Wet-synthesized hydroxyapatite as the control was prepared according to a previous study[19].

FTIR Analysis

The Fourier transform infrared (FTIR) analyses of the cortical and cancellous bone powders were performed with a Perkin-Elmer 6 000 FTIR spectrometer (Perkin Elmer Co., USA) in a wave-number range of 500-4 000 cm^{-1}, using the transmission spectroscopy method.

Chemical Analysis

The contents of Ca and P in samples were measured by wet chemical method. Samples were dissolved in concentrated HNO_3/HCl solution. The amount of Ca was determined by complex-ometric titration with EDTA in alkaline solution of KOH (pH

⩾12.5). The amount of P was measured indirectly by phosphomolybdate technique. The solution was boiled and precipitator was added. The amount of P was conversed by the mass of the precipitation. The procedure was according to China Standard GB/T 1871.1-1995.

XPS Analysis

XPS analysis was conducted on a Kratos XSAM800 X-ray Photoelectron Spectrometer (KRATOS, England) with a double anode Mg-Ka-X-ray (1253.6 eV) and a detector. A concentric hemispherical analyzer was operated in the constant analyzer transmission mode to measure the binding energies of emitted photoelectrons. The binding energy scale was calibrated by the Ag3d5/2 peak at 368.3 eV, and the linearity was verified by the Cu2p3/2 peak at 932.7 eV, respectively. Survey spectra were collected from 0 to 1 100 eV, and middle-resolution spectra were collected for C1s, N1s and Ca2p peaks. All spectra were referenced by setting the hydrocarbon C1s peak to 284.8 eV to compensate for residual charging effects. Data for percent atomic composition and atomic ratios were calculated using the manufacturer- supplied software.

RESULTS AND DISCUSSIONS

SEM Micrographs

The SEM micrographs of cortical and cancellous bone are shown in Fig. 1. It can be seen in Fig. 1 (a, b) that the collagen fibers of cortical bone were arrayed more orderly than those of cancellous bone, and the mineralized fibers looked similar as shown in Fig. 1(c, d).

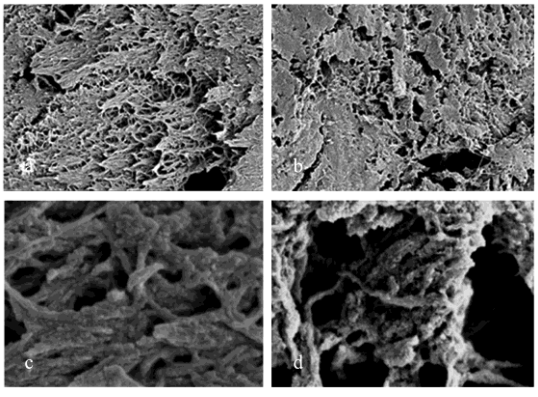

FIG. 1. SEM photographs of the cortical bone (a, c) and cancellous bone (b, d).

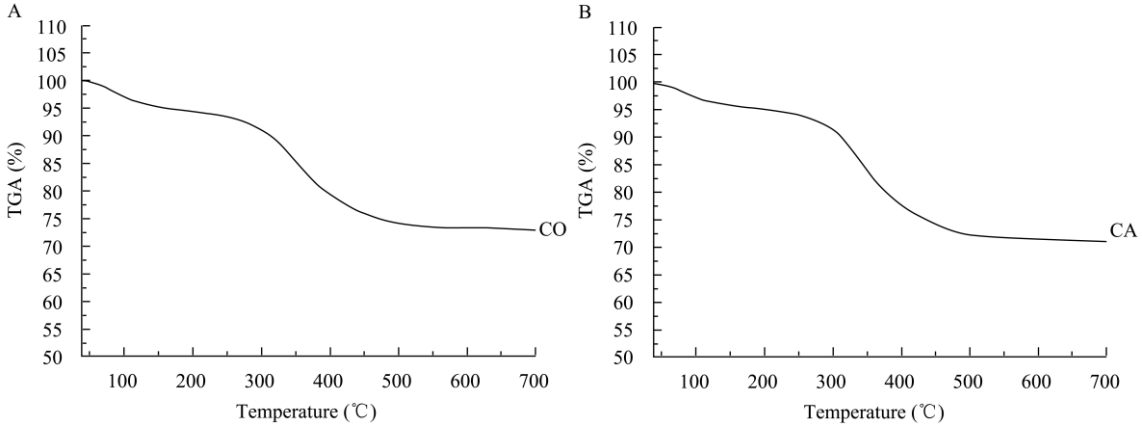

FIG. 2. TG curves of the cortical bone (CO) and cancellous bone (CA) from the room temperature to 700 ℃.

TG Curves

Figure 2 shows the TG curves of cortical bone (CO) and cancellous bone (CA) heated from the room temperature to 700 ℃. The first stage of weight loss from 60 ℃ to 250 ℃ represents the dehydration process. Mostly the adsorbed and loosely bound water removes from surface of samples. The second stage corresponding to the fast weight loss appears in the temperature range from 250 ℃ to 450 ℃, indicating a process of degradation and combustion of organic components, especially the collagen fibers, as well as the release of some strongly bounded crystal water. At the third stage from 450 ℃ to 700 ℃, the weight loss rate decreases and the weight loss is very slow above 550 ℃. The weight loss at this stage should be the volatilization of lattice carbonate and the release of possible lattice water. The TG curve or the trend of weight loss for both cortical bone and cancellous bone looks similar, but the amount of weight loss at each stage is somewhat different. For cortical bone, the weight loss is 6.7% at the first stage, 17.4% at the second stage and 2.7% at the third stage. This process is similar to the TG plot reported by Enzo *et al.*[20] who

studied ancient human bone mainly referring to the cortical bone. However, the weight loss for the cancellous bone is 5.8%, 19.9 %, and 2.8% at each stage. As a result, the mineral content in cortical bone and cancellous bone is 73.2wt% and 71.5wt% respectively and the former is a little higher than the latter.

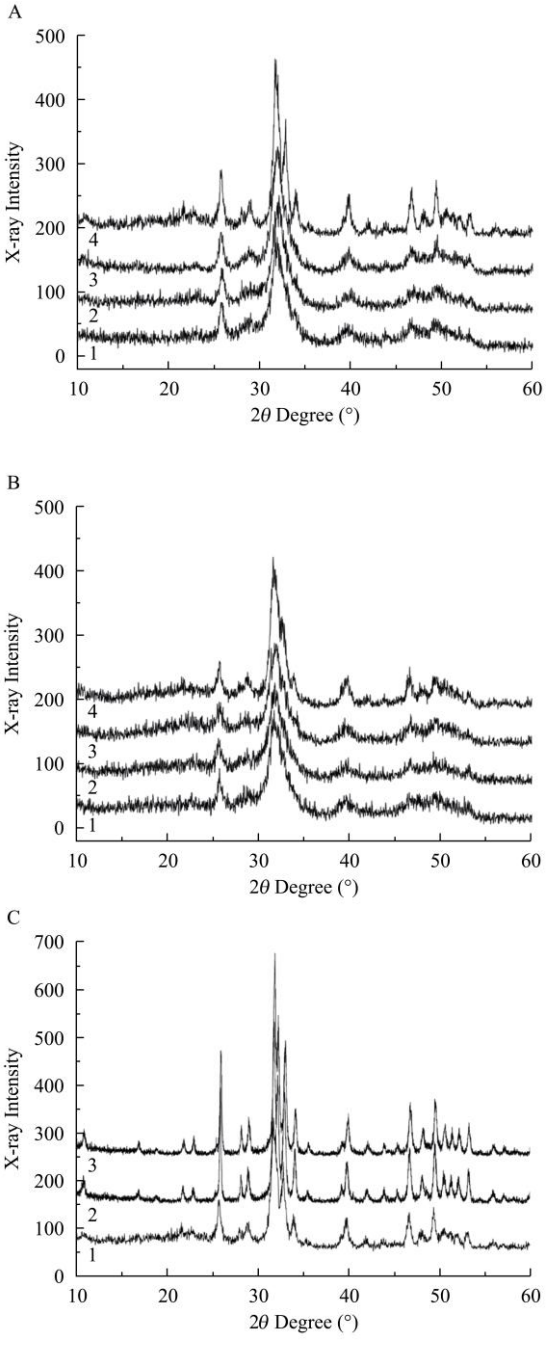

FIG. 3. XRD patterns of cortical bone (A): (1) CO, (2) CO250, (3) CO450, (4) CO650; cancellous bone (B): (1) CA, (2) CA250, (3) CA450, (4) CA650; and 650 ℃ comparison (C): (1) CO650, (2) CA650, (3) synthetic HA sintered at 650 ℃.

XRD Patterns

Figure 3 shows the XRD patterns obtained from the cortical and cancellous bone. Before heat treatment, both cortical and cancellous bone present a typical poorly crystallized XRD pattern of HA in a hexagonal symmetry (ref.: JCPDS no.9-432). The peaks at 2θ = 25.8 °(002), 28.1 °(102), 29 °(210), 31.8 °(211), 32.9 °(300), 34.1 °(202), 39.6 °(310), 46.7 °(222), 49.5 °(213) and 53.2 °(004) exist in all samples. The peak intensity or crystallinity of these bone samples increases with the temperature of heat treatment, but the increase is not obvious below 650 ℃ as shown in Fig. 3(A, B). When treated at 650 ℃, the crystallinity of cortical bone (i.e., the cortical bone apatite) is more similar to that of the synthetic HA, both are higher than that of cancellous bone. The better crystallinity reflects the greater regularity of atomic arrangement, if the crystal size of cortical bone apatite is not larger than that of cancellous bone apatite.

The diffraction peaks of both bone samples before heat treatment or dehydration are broad and diffuse, indicating the low crystallization degree of bone apatite crystals which are in nano range with very small crystal size. The XRD patterns of both cortical and cancellous bone exhibit no obvious change at room temperature, 250 ℃ and 450 ℃. This means that the adsorbed water and loosely bounded water have little influence on the crystal structure of bone apatite. When the treating temperature increases from 450 ℃ to 650 ℃, the peak intensity or crystallinity of bone apatites enhances obviously, mainly ascribed to the growth and rearrangement of apatite crystals and partly due to the complete disappearance of collagen fibers and the release of lattice carbonate groups and lattice water. The loss of lattice carbonate or water could certainly promote the lattice rearrangement and change the size of the bone apatite crystals (the distance between neighboring lattice sites is affected) as has been observed in dehydrated enamel and precipitated apatites[14]. This result agrees with the finding of Hiller *et al.*[21-22] by X-ray scattering technology and that of Benmarouane *et al.*[23] by neutron diffraction to study bone change during experimental heating.

A semi-quantitative relationship between peak width and crystallite size *D* (diameter of the coherently scattering domains) is given by the Scherrer equation[24]. Since in bioapatite crystals, the largest dimension is usually parallel to the *c*-axis, the variations in (002) data are related to lattice parameters along the crystal length. Therefore, the characteristic peak at 25.8 ° for (002) plane was used to calculate the size of apatite crystals, according to the Scherrer formula $D = k\lambda / (\beta_{1/2} \cos\theta)$ where *D* is the average crystal size; *k* is a constant depending on

crystal habit (here chosen as 0.89); λ is the wavelength of X-ray radiation (1.542 Å); $\beta_{1/2}$ is the half width of the diffraction peak (rad); and θ (°) is Bragg angle. The half width of the instrument is taken into account, giving a value of 0.0937. The apatite lattice parameters and average crystal size of different samples calculated using XRD data are shown in Table 1.

It can be seen from Table 1 that the apatite crystal size of both cortical bone and cancellous bone is in nano scale (about 17-18 nm) and increases gradually with the treating temperature. The apatite lattice parameters of *a* and *c* in all samples are slightly smaller than that of synthetic HA. The process of heat treatment causes an extension in the *a*-lattice parameter and changes the *c*-lattice parameter without regular pattern. This is usually associated with an increase in the crystallinity, reflecting lattice rearrangement after the release of lattice carbonate and lattice water and an increase of crystal size, imparting greater stability to the structure. The fact has also been confirmed by Rogers[15] and Pasteris[25].

IR Spectra

Lebon[26] and Thompson[27] have studied bones using Fourier transform infrared spectrometry and monitored the changes of FTIR spectral features relating to the evolution of mineral properties. The IR spectra obtained from our samples of cortical and cancellous bone are shown in Fig. 4 (A, B). All the samples show the following apatite characteristic bands: 1 028-1 100 cm^{-1} (*v*3, P-O stretch), -960 cm^{-1} (*v*1 sym, P-O stretch), -603 cm^{-1} (*v*4, P-O stretch), -564 cm^{-1} (*v*4, P-O stretch and P-O bending). The bands at 1 630-1 660 cm^{-1} are related to organic tissue and water, the band intensity decreases with the treating temperature. The broad bands around 3 400 cm^{-1} are attributed to water. The peaks at 3 573 cm^{-1} and 632 cm^{-1} in Fig. 4A belong to the OH stretching mode of apatite.

The bands from 1 400-1 550 cm^{-1} and the peak at 874 cm^{-1} can be assigned to CO_3^{2-} groups according to previous reports[28-29]. After heat treatment above 450 ℃, the organic components in bone samples have been fully removed, the residual bands around 1 630-1 650 cm^{-1} can be only assigned to water, and the bands from 1 400-1 550 cm^{-1} and the peak at 874 cm^{-1} should be only caused by lattice carbonate groups.

It can be seen from Fig. 4C that both the bone apatite and the synthetic hydroxyapatite contain the vibration bands of phosphate groups, hydroxyl groups and water, and the synthetic HA holds higher crystallinity as shown by the clear band-splitting at 1 030-1 100 cm^{-1}. However, the synthetic HA does not show the vibration of carbonate groups, and the water band intensity of bone apatites is higher than that of synthetic HA. The X-ray diffraction pattern (Fig. 3) and infrared spectra (Fig. 4) indicate that the apatite of animal origin can preserve its HA structure via heat treatment, which is in agreement with the report by Haberko *et al.*[30].

Chemical Analysis

The content of Ca and P and the Ca/P molar ratio are listed in Table 2. The Ca/P ratio of cortical bone is 1.69 which is higher than that (1.67) of stoichiometric HA. The biological apatite is always carbonate substituted, the location of CO_3^{2-} groups on the phosphate site in apatite lattice can explain why the value of Ca/P ratio is higher than 1.67. There is general agreement that the carbonate ions can substitute both for the OH groups (Type A substitution) and the phosphate groups (Type B substitution) in the apatite crystal structure[2], and these structural substitutions will result in characteristic IR signatures: Type A carbonate substitution produces a doublet bands at about 1 545 and 1 450 cm^{-1} (asymmetric stretching vibration, *v*3) and a singlet band at 880 cm^{-1} (out-of-plane bending vibration, *v*2), and Type B carbonate substitution has bands at about 1 455, 1 410, and 875 cm^{-1} respectively. The IR peak at 875 cm^{-1} in Fig. 4C (1, 2) indicates that the minerals of both cortical and

TABLE 1
Apatite Crystal Size *D* (nm) and Lattice Parameters Calculated from High-Resolution XRD Using the Scherrer Equation

Sample	Lattice Parameters (Å)		Crystal Size *D* (002) (nm)
	a	*c*	
CO	9.39474	6.87902	17.48
CO250	9.39549	6.87923	18.02
CO450	9.40791	6.87652	19.76
CO650	9.41094	6.88102	20.63
CA	9.40493	6.87512	17.08
CA250	9.40702	6.88138	18.14
CA450	9.41019	6.87807	19.87
CA650	9.41235	6.87406	21.02
Synthetic HA	9.41433	6.88096	29.21

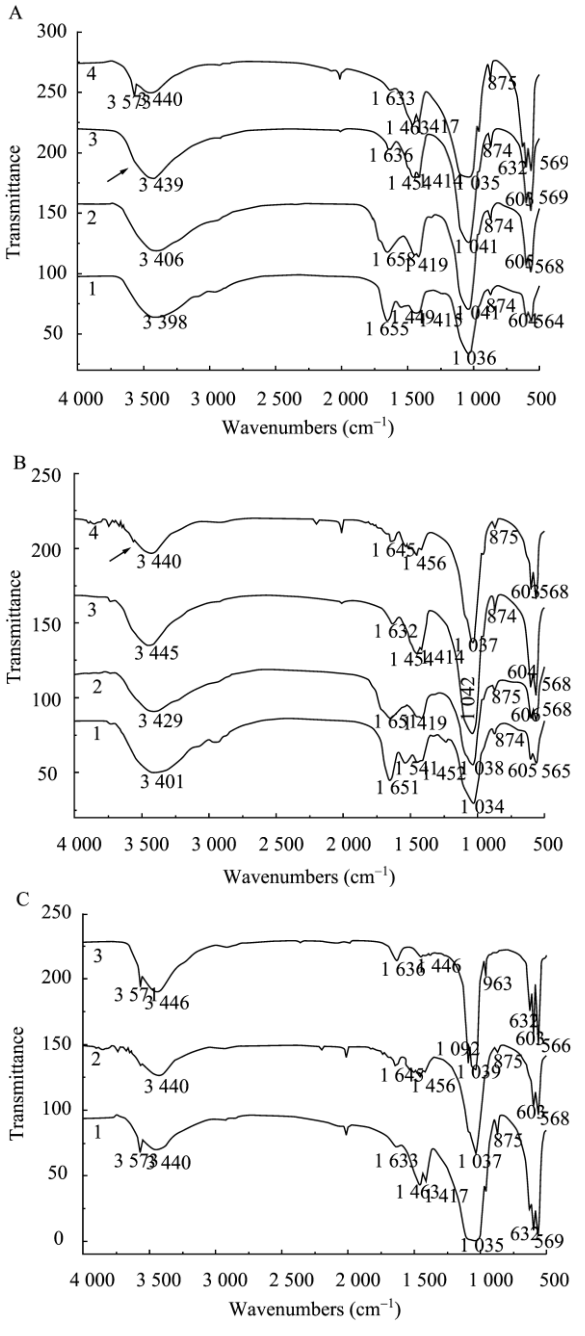

FIG. 4 IR spectra of cortical bone (A): (1) CO, (2) CO250, (3) CO450, (4) CO650; cancellous bone (B): (1) CA, (2) CA250, (3) CA450, (4) CA650; and 650 ℃ comparison (C): (1) CO650, (2) CA650, (3) synthetic HA sintered at 650 ℃.

cancellous bone are carbonate-substituted apatite. Carbonate substitution can cause crystal disorder, resulting in decrease of apatite crystallinity that is one of the reasons why biological apatites are poorly crystallized. The fact that Ca/P ratio of cortical bone is higher than that (1.65) of cancellous bone may result from more Type B CO_3^{2-} substitution in cortical bone than in cancellous bone, which is in accordance with the higher peak intensity at 875 cm^{-1} of cortical bone [Fig. 4C(1)]. The Ca/P ratio of cancellous bone is lower than 1.67 of stoichiometric HA, suggesting that the apatite in cancellous bone is a kind of more calcium deficient apatite.

TABLE 2

The Content of Ca, P, and Ca/P Molar Ratio

Sample	Ca (%)	P (%)	Ca/P
CO650	38.01	17.43	1.69
CA650	37.12	17.36	1.65

XPS Spectra

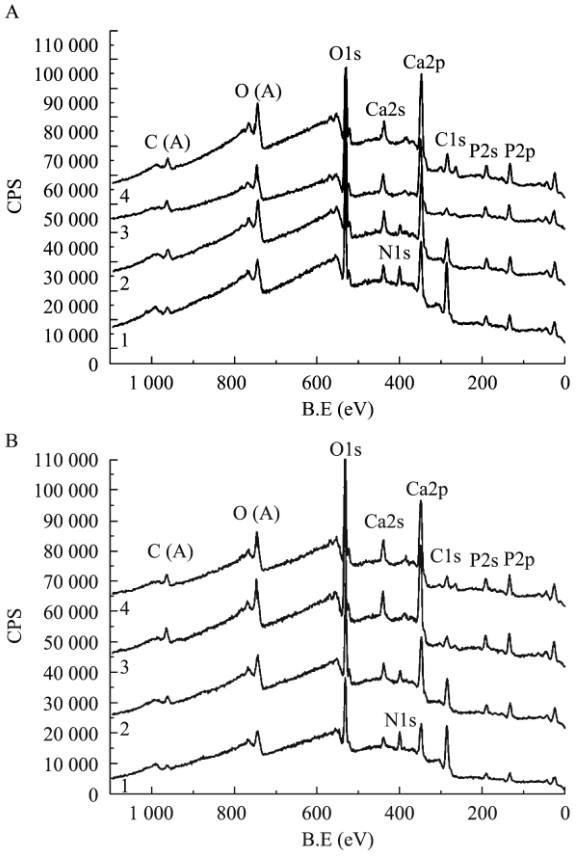

FIG. 5. XPS spectra of cortical bone (A): (1) CO, (2) CO250, (3) CO450, (4) CO650 and cancellous bone (B): (1) CA, (2) CA250, (3) CA450, (4) CA650.

Figure 5A shows the XPS spectra of the cortical bone samples having major peaks associated with C1s, Ca2p, P2p, N1s and O1s at 285, 347, 133, 400, and 531 eV, respectively. The XPS spectra of cancellous bone are similar to the major peaks of cortical bone. It should be noted that the intensity of

N1s peak at 400 eV decreases with treating temperature and the peak disappears above 450 ℃, and although the C1s peak also decreases with the treating temperature, it still exists even above 450 ℃, as shown in Fig.5A(3, 4) and Fig.5B(3, 4). This indicates that the organic component such as protein and collagen has been fully removed above 450 ℃ and lattice carbonate groups are present in the apatite.

Table 3 gives the element binding energy of cortical and cancellous bone treated at different temperatures. The difference of binding energies for Ca, P, O elements is less than 0.6 eV, indicating slightly change or modification in chemical environment of apatite structure. This is in agreement with the rearrangement of apatite crystal structure during heat treatment. The binding energy of N element is similar below 250 ℃ and no data are detected above 450 ℃.

TABLE 3

The Element Binding Energy of Cortical Bone and Cancellous Bone at Different Treating Temperature.

	CO	CO 250	CO 450	CO 650	CA	CA 250	CA 450	CA 650
Ca	347.0	346.9	347.3	347.0	347.1	347.4	347.5	347.2
P	133.2	133.1	133.6	133.3	133.5	133.8	133.6	133.5
O	530.8	530.8	531.1	530.9	530.9	531.2	531.2	531.0
N	399.6	399.6	0.0	0.0	399.6	399.9	0.0	0.0

CONCLUSION

The finding s from this study demonstrated that after the removal of the organic component such as protein and collagen above 450 ℃, lattice carbonate groups were present in the apatite crystal structure. The minerals in both cortical and cancellous bone were composed of poorly crystallized nano-size apatite crystals with lattice carbonate and possible lattice water. The mineral content in cortical bone was slightly higher than that in cancellous bone. The adsorbed water and loosely bounded water had little influence on the crystal structure of bone apatite. However, the effect of the release of lattice carbonate and water on crystallographic properties of cortical and cancellous bone was obvious. For design and preparation of bone biomaterials, the inorganic component should mimic the composition and crystal structure of bone apatite. The result is helpful for future biomaterial design, preparation and application. And, further study should focus on the determination of lattice water and the function of lattice water on the growth of biological apatite crystals.

ACKNOWLEDGEMENTS

The authors expressed their sincere thanks to Prof. Hong Chen and Shuxing Xiao of the Sichuan University for their strong supports in data collection and analysis.

REFERENCES

1. Hench L L, Wilson J (1993). *An Introduction to Bioceramics*, ed. pp. 145. World Scientific Publishing Co, Singapore.
2. Fleet M E, Liu X-J (2003). Carbonate apatite type A synthesized at high pressure new space group (P3) and orientation of channel carbonate ion. *Journal of Solid State Chemistry* **174**, 412-417.
3. Nyman J S, Roy A, Shen X M, *et al*. (2006). The influence of water removal on the strength and toughness of cortical bone. *J Biomech* **39**, 931-938.
4. Peters F, Schwarz K, Epple M (2000). The structure of bone studied with synchrotron X-ray diffraction, X-ray absorption spectroscopy and thermal analysis. *Thermochimica Acta* **361**, 131-138.
5. Dalconi M C, Meneghini C, Nuzzo S, *et al.* (2003). Structure of bioapatite in human foetal bones: An X-ray diffraction study. *Nuclear Instruments and Methods in Physics Research B* **200**, 406–410.
6. Utku F S, Klein E, Saybasili H, *et al.* (2008). Probing the role of water in lamellar bone by dehydration in the environmental scanning electron microscope. *Journal of Structural Biology* **162**, 361-367.
7. Nomura S, Hiltner A, Lando J B, *et al.* (1977). Interaction of water with native collagen. *Biopolymers* **16**, 231-246.
8. Wilson E E, Awonusi A, Morris M D, *et al.* (2005). Highly Ordered Interstitial Water Observed in Bone by Nuclear Magnetic Resonance. *J Bone Miner Res* **20**, 625-634.
9. Wilson E E, Awonusi A, Morris M D, *et al.* (2006). Three Structural Roles for Water in Bone Observed by Solid-State NMR. *Biophysical Journal* **90**, 3722-3731.
10. Ni Q W, Nyman J S, Wang X D, *et al.* (2007). Assessment of water distribution changes in human cortical bone by nuclear magnetic resonance. *Meas. Sci. Technol* **18**, 715-723.
11. Nyman J S, Ni Q W, Nicolella D P, *et al.* (2008). Measurements of mobile and bound water by nuclear magnetic resonance correlate with mechanical properties of bone. *Bone* **42**, 193-199.
12. Timmins P A, Wall J C (1977). Bone Water. *Calcif Tissue Res* **23**, 1-5.
13. Nyman J S, Roy A, Shen X M, *et al.* (2006). The influence of water removal on the strength and toughness of cortical bone. *J Biomech* **39**, 931-938.
14. LeGeros R Z, Bonel G, LeGros R (1978). Type of 'H_2O' in human enamel and precipitated apatites. *Calcif Tissue Res* **26**, 111-118.
15. Rogers K D, Daniels P (2002). An X-ray diffraction study of the effects of heat treatment on bone mineral microstructure. *Biomaterials* **23**, 2577-2585.
16. Danilchenko S N, Koropov A V, Protsenko I Y, *et al.* (2006). Thermal behavior of biogenic apatite crystals in bone: An X-ray diffraction study. *Cryst Res Technol* **41**, 268-275.
17. Ooi C Y, Hamdi M, Ramesh S (2007). Properties of hydroxyapatite produced by annealing of bovine bone. *Ceramics International* **33**, 1171-1177.
18. Piga G, Malgosa A, Thompson T J U, *et al.* (2008). A new calibration of the XRD technique for the study of

archaeological burned human remains. *Journal of Archaeological Science* **35**, 2171-2178.
19. Wang X J, Li Y B, Wei J, *et al* (2002). Development of biomimetic nano-hydroxyapatite/poly (hexamethylene adipamide) composites. *Biomaterials* **23**, 4787-4791.
20. Enzo S, Bazzoni M, Mazzarello V, *et al.* (2007). A study by thermal treatment and X-ray powder diffraction on burnt fragmented bones from tombs II, IV and IX belonging to the hypogeic necropolis of ''Sa Figu'' near Ittiri, Sassari (Sardinia, Italy). *Journal of Archaeological Science* **34**, 1731-1737.
21. Hiller J C, Thompsonb T J U, Evison M P, *et al.* (2003). Bone mineral change during experimental heating: an X-ray scattering investigation. *Biomaterials* **24**, 5091-5097.
22. Hiller J C, Wess T J (2006). The use of small-angle X-ray scattering to study archaeological and experimentally altered bone. *Journal of Archaeological Science* **33**, 560-572.
23. Benmarouane A, Hansena T, Lodini A (2004). Heat treatment of bovine bone preceding spatially resolved texture investigation by neutron diffraction. *Physica B* **350**, e611–e614.
24. Kaelble E F (1967). Handbook of X-rays, ed. McGraw-Hill, New York, USA.
25. Pasteris J D, Wopenkaa B, Freeman J J, *et al*. (2004). Lack of OH in nanocrystalline apatite as a function of degree of atomic order: implications for bone and biomaterials. *Biomaterials* **25,** 229-238.
26. Lebon M, Reiche I, Bahain J J, *et al.* (2010). New parameters for the characterization of diagenetic alterations and heat-induced changes of fossil bone mineral using Fourier transform infrared spectrometry. *Journal of Archaeological Science* 1-12.
27. Thompson T J U, Gauthier M, Islama M (2009). The application of a new method of Fourier Transform Infrared Spectroscopy to the analysis of burned bone. *Journal of Archaeological Science* **36**, 910-914.
28. Elliot J C (1994). Structure and chemistry of the apatites and other calcium orthophosphates. first edition, Amsterdam: Elsevier.
29. Antonakos A, Liarokapis E, Leventouri T (2007). Micro-Raman and FTIR studies of synthetic and natural apatites. *Biomaterials* **28**, 3043-3054.
30. Haberko K, Bućko M M, Brzezińska-Miecznik J, *et al.* (2006). Natural hydroxyapatite-its behaviour during heat treatment. *Journal of the European Ceramic Society* **26**, 537-542.

(*Received January* 26, 2010 *Accepted October* 11, 2010)